

An evaluation of spherical designs for molecular-like surfaces

Richard J. Morris

John Innes Centre, Norwich Research Park, Colney, NR4 7UH Norwich, UK

Received 4 August 2005; accepted 3 October 2005

Available online 7 November 2005

Abstract

The use of spherical harmonics in the molecular sciences is widespread. They have been employed with success in, for instance, the crystallographic fast rotation function, small-angle scattering particle reconstruction, molecular surface visualisation, protein–protein docking, active site analysis and protein function prediction. The calculation of spherical harmonic expansion coefficients requires integration over the full sphere and can be a computationally cumbersome and also numerically sensitive (with respect to the integration weights) procedure. It is shown here how the use of spherical *t*-designs and pre-computed near-equal weight integration layouts can significantly reduce the computational effort in the determination of spherical harmonic expansion coefficients for molecular surfaces, thus giving rise to a robust and highly efficient algorithm for the construction of molecular-like objects.

© 2005 Elsevier Inc. All rights reserved.

Keywords: Molecular surfaces; Spherical harmonics; Cubature

1. Introduction

Evidence is accumulating to suggest that the concept of molecular surfaces is in many cases only meaningful when all interaction partners are considered. This is due to the flexible nature of protein structures and induced conformational changes during complex formation [1]. The study of static molecular surfaces of isolated small molecules, proteins and other macromolecules, however, remains a very popular and powerful approach to address questions concerning molecular recognition and functional analysis. Several methods have been developed for this purpose. Spherical harmonics have been used for the visualisation of molecular surfaces [2,3] and more recently, developments have elegantly extended the method to enable shape and charge comparisons for protein–protein docking [4,5]. Following the original work of Ritchie and Kemp [4], spherical harmonic expansion coefficients have been used to directly describe and compare the shapes of binding pockets for virtual screening [6,7]. The main advantages of using spherical harmonics are that the method is analytical with a clear control on the level of detail, has relatively few parameters, it is unique in that different shapes have different expansion coefficients, and it allows for physical-chemical properties to be described within the same framework. The use

of spherical harmonics in the molecular sciences is, therefore, widespread [2–21].

Harmonics are solutions of Laplace's equation. Spherical harmonics are solutions to the angular part of Laplace's equation in spherical coordinates (r, θ, ϕ) and can be defined as

$$Y_{lm}(\theta, \phi) = \sqrt{\frac{2l+1}{4\pi} \frac{(l-m)!}{(l+m)!}} P_{lm}(\cos \theta) \exp(im\phi) \quad (1)$$

where l and m ($-l \leq m \leq +l$) are function indices and P_{lm} associated Legendre polynomials. Spherical harmonics form a complete set of orthonormal functions on the unit sphere, S_2 . Thus, any function f on S_2 expressed in spherical coordinates, $(\phi, \theta) \in [0, 2\pi) \times [0, \pi]$, can be represented exactly as a series of spherical harmonics,

$$f(\theta, \phi) = \sum_{l=0}^{\infty} \sum_{m=-l}^l c_{lm} Y_{lm}(\theta, \phi). \quad (2)$$

The computation of the expansion coefficients, c_{lm} , requires integration over the solid angle Ω on the full sphere S_2 of the function being represented, f , and the complex-conjugate spherical harmonic of the same indices, l and m ,

$$c_{lm} = \int_{S_2} f(\theta, \phi) Y_{lm}^*(\theta, \phi) d\Omega. \quad (3)$$

E-mail address: Richard.Morris@bbsrc.ac.uk.

Analytical expressions for the surface of molecules exist, but typically the integration is carried out numerically. Numerical multidimensional integration is far from trivial—see [22] for a brief discussion and references within for further details—and can be a time-consuming and error-prone procedure. The complexity of this numerical integration is proportional to the number of sample points used. Also, the ease with which the cubature weights can be computed is highly dependent on the number of chosen points, due to the multi-minima nature of the typical objective functions used for their determination.

The Nyquist–Shannon sampling theorem states that to resolve features of frequency ν one must sample at, at least, 2ν . The same argument applies in Fourier space, so to resolve spatial features of a given distance, one must sample at half that distance. To represent atomic details of proteins can, therefore, require a very large number of surface sample points, depending, of course, on the total surface area. Faithfully reproducing these atomic details with spherical harmonics makes an expansion to high order of l necessary, often well above 40. However, for visualisation purposes and even more so for shape-matching it is often sufficient to terminate the expansion below 16. We found that for shape classification, $l_{\max} = 8$ often provided adequate detail, see [7] and Figs. 1 and 2, which show the reconstruction of two molecules using a spherical harmonic approximation. Unless the expansion is really required to higher orders, sampling the surface in the detail in which it is commonly performed by standard integration techniques (often many thousands of sample points) is rarely justified.

For the development of a fast shape-matching method [7], we needed to evaluate the quality of our shape approximations. The integration step for the determination of the expansion coefficients can play a crucial role in the performance, both in execution time and numerical accuracy. In this article, a comparison over a large set of optimal and near-optimal cubature formulae is presented for a number of molecular surfaces generated at various degrees of resolution.

2. Spherical cubature formulae

One method for the computation of spherical harmonic expansion coefficients requires a least-square fit to a set of points obtained from over-sampling (relative to the sufficient Nyquist–Shannon frequency) the surface [2,6]. For cases in which the data are not too noisy or an over-sampling of the surface is not practical, a more elegant approach for the computation of the expansion coefficients exists. This approach

follows Eq. 3 and involves the numerical integration of the function to be expanded over S_2 . Numerical integration on the sphere is straightforward, in principle, following standard integration procedures. The implementation, however, reveals a number of difficulties and with insufficient care for the details, this step can become highly sensitive towards the integration sample points and their weights as well as becoming unnecessarily time consuming. Cubature formulae for the sphere have therefore deservedly been given dedicated research focus. By cubature formulae we mean a set of points with the appropriate weights such that an integral over this space can be computed by a weighted sum of point evaluations.

The problem of finding good cubature formulae on the sphere [23] is related to Fejes Tóth's and Thomson's problem, the facility dispersion problem and multivariate Gaussian quadrature. Fejes Tóth's problem addresses how N points can be distributed on the unit sphere such that they maximise the minimum distance between any pair of points. Thomson's problem may be described as how to determine a stable equilibrium of N point charges constrained on the surface of a sphere. The inverse square charge repulsion forces the charges to also maximise the minimum distance between any two points. Although mathematically equivalent to Tóth's problem, a physical system of point charges cannot be held in stable equilibrium by their electrostatic interactions alone. This is known as Earnshaw's theorem. Despite their apparent simplicity and broad range of applications, these are in general still unsolved problems.

An arrangement of N points on a sphere that corresponds to the placement of N identical non-overlapping spheres around another sphere is called a sphere packing. The configuration of such points is called a spherical code. The number of spheres that touch an equivalent sphere is called the kissing number. See [24] for an introduction to sampling methods and the references within for more in-depth presentations.

A spherical design of strength t (spherical t -design) describes the placement of N points on the unit sphere such that all points have equal numerical integration weights [25]. Mathematically, a set of points, $X = \{\mathbf{p}_1, \mathbf{p}_2, \dots, \mathbf{p}_N\}$, is a spherical t -design on S_{d-1} if and only if it is possible to exactly determine the average value on S_{d-1} of any polynomial f of degree at most t by sampling f at the points of X ,

$$\int_{S_{d-1}} f(\mathbf{x}) d\mu(\mathbf{x}) = \frac{1}{N} \sum_{i=1}^N f(\mathbf{p}_i). \quad (4)$$

S_{d-1} is the $(d-1)$ -dimensional surface of a unit sphere in d dimensions and $\mu(\mathbf{x})$ is a uniform normalised measure on the

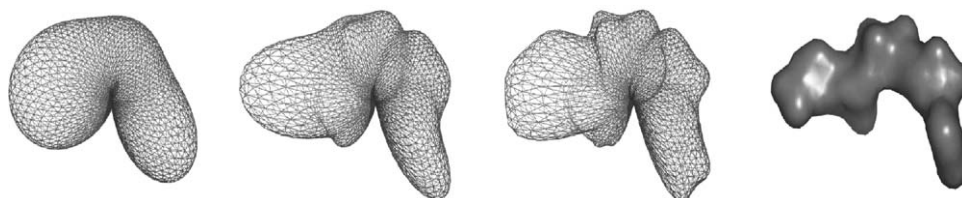


Fig. 1. Spherical harmonic approximations to the shape of nicotinamide adenine dinucleotide (NAD) in a given conformation. From left to right, $l_{\max} = 4$, $l_{\max} = 8$, $l_{\max} = 16$, and the van der Waals surface. Images produced with Pymol [32].

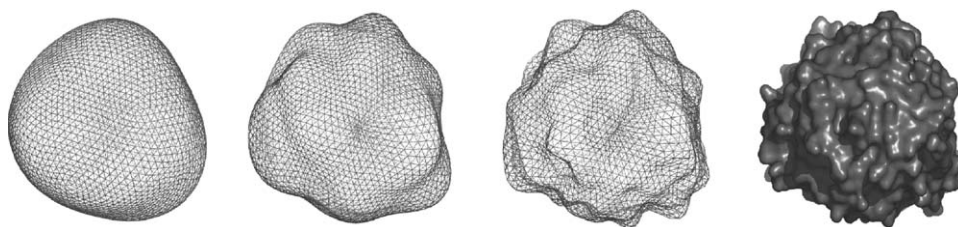


Fig. 2. Spherical harmonic approximations to the shape of endoglucanase CelA (PDB ID 1is9, [30]). From left to right, $l_{\max} = 4$, $l_{\max} = 8$, $l_{\max} = 16$, and the van der Waals surface. Images produced with Pymol [32].

sphere S_{d-1} . Although spherical t -designs are proven to exist only for rather low degrees, (up to $t = 12$ corresponding to $N \geq 48$ sample points), there is strong numerical evidence to suggest that point layouts can be found up to $t = 21$ with equal weights [26].

Fliege and Maier [27] have explored cubature formulae that are not spherical t -designs but have near-equal weights. Relaxing the strict requirement for equal integration weights allows significantly higher orders to be explored. Fliege and Maier have published point sets on S_2 up to $N = 900$. They use a two-stage approach to determine the points and their weights. First, a good approximation of the multi-minima Thomson problem is sought using simulated annealing. The resulting configuration is then fine-tuned using the L-BFGS algorithm and the weights are calculated. A similar approach can be found in Morris et al. [28] that uses a genetic algorithm.

When studying only one function at a time on S_2 , some cubature formulae perform astonishingly well and are often capable of achieving individual accuracies of the same order of magnitude as machine precision for the integration of simple functions on the sphere. However, for spherical harmonic expansions one is faced with an additional complication in that to reconstruct surface points, one requires not one integration on the sphere but $\sum_{l=0}^{l_{\max}} (2l+1)$ expansion coefficients. A few small errors in only some of these coefficients can quickly accumulate into large errors. Therefore, an evaluation of any cubature formula for molecular surfaces should be based on a full image reconstruction and not individual coefficient accuracies as these can be misleading.

3. Results

We have performed the following experiment to test the integration layouts of Hardin and Sloane [26] and Fliege and Maier [27]. We first expanded various molecular surfaces (proteins and ligands), as defined by their solvent accessible surface area, in real spherical harmonics up to $l_{\max} = 20$. We then applied a high-frequency filter to lose the finer details by setting the coefficients above a chosen l_{\max} to zero. This was performed in the l_{\max} range of 4–20. For each of these medium to low resolution molecular surfaces, we tested the full range of integration schemes—18 spherical t -designs ranging from 16 to 240 points proposed by Hardin and Sloane [26] and 26 spherical designs ranging from 16 to 841 points proposed by Fliege and Maier [27]—to evaluate the accuracy with which these shapes could be expanded in spherical harmonics and reconstructed

from their coefficients that were computed with each integration layout.

We evaluated the accuracy of the cubature formulae by computing the summed squared differences between the reconstructed molecular surfaces from the terminated original expansion and those computed from the coefficients obtained using the cubature formulae,

$$\frac{1}{N} \sum_{i=1}^N (r_{\text{original}} - r_{\text{reconstructed}})^2. \quad (5)$$

These values were computed at 900 sample points that were not used during integration. To eliminate size bias, we normalised all expansion coefficients by the first spherical harmonic expansion coefficient prior to the reconstruction. This is equivalent to normalising the mean square error by the radius of the molecule (zeroth order shape approximation), thus making the units equal to $\text{\AA}^2/\text{\AA}=\text{\AA}$. This normalisation procedure produces remarkably consistent curves, see Figs. 3 and 4, which were calculated for ligands and proteins, respectively, for the spherical t -designs of Hardin and Sloane [26]. These plots show the normalised mean square error between the original surface of degree l_{\max} and the reconstructed surface from a spherical harmonics expansion computed using various cubature formulae versus the expansion order. These plots highlight the situations in which the designs deviate from the exact solution. Given an acceptable average error tolerance, zooming in on such plots allows one to choose the optimal (minimal number of points for a given error tolerance) integration layout, Fig. 5. In Fig. 3, the original surface was computed from nicotinamide adenine dinucleotide, NAD, (taken from 1heu, [29]). Fig. 4 shows a similar plot calculated using the molecular surface from Endoglucanase CelA (taken from 1is9, [30]). Fig. 6 shows an evaluation of the Fliege and Maier [27] integration nodes. These plots show that impressive normalised mean square errors in the region of 10^{-5}\AA are achievable all the way up to $l_{\max} = 20$ with not much more than a few hundred integration points.

The consistency of such normalised plots allows one to make approximate predictions for the quality of any molecular surface reconstruction with spherical harmonics for a given order and chosen cubature formula. If, for instance, the normalised mean square deviation for a given order l_{\max} and a chosen integration layout was 0.01\AA and the size of the protein under study was of radius 20\AA (more precisely, if the first harmonic expansion coefficient of this protein was 20\AA),

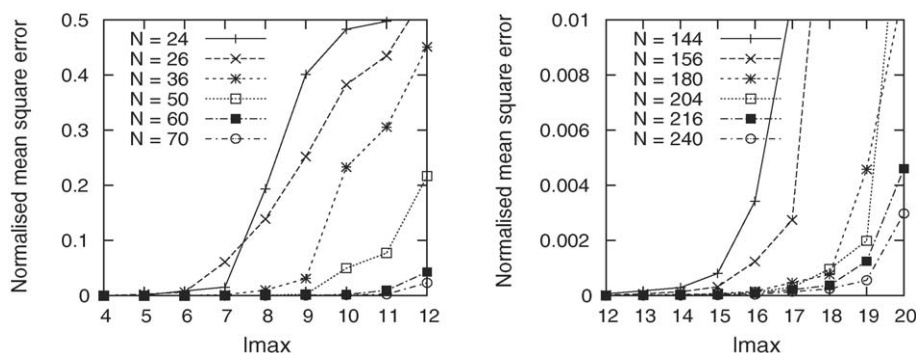


Fig. 3. The quality of spherical t -designs [26] for spherical harmonic expansions for the small molecule NAD. The normalised mean square error between the original surface of degree l_{\max} and the reconstructed surface from a spherical harmonics expansion using various cubature formulævs. the expansion order is shown. N is the number of points of the spherical designs.

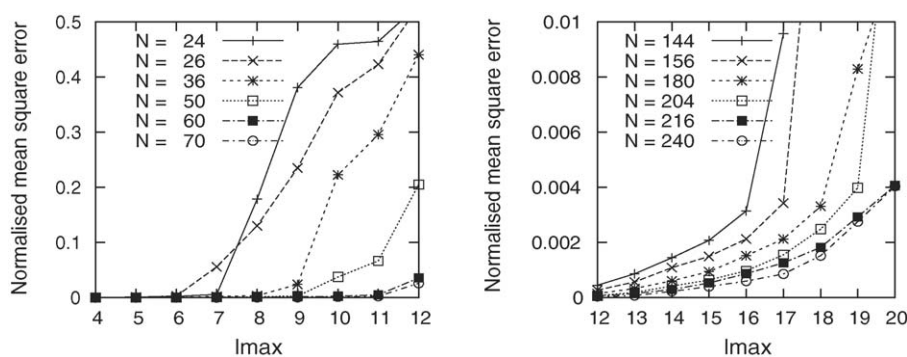


Fig. 4. The quality of spherical t -designs [26] or spherical harmonic expansions for the protein CcIA. The normalised mean square error between the original surface of degree l_{\max} and the reconstructed surface from a spherical harmonics expansion using various cubature formulævs. the expansion order is shown. N is the number of points of the spherical designs.

then one would expect a mean square deviation between the reconstructed and the original protein surface of $0.01 \text{ \AA} \times 20 \text{ \AA} = 0.2 \text{ \AA}^2$. Deviations from such approximations indicate that the star-shape requirement is poorly satisfied [7].

Closer examination of the data used to produce these plots shows some, perhaps unexpected, dips in the curves. For example, in Figs. 3 and 4, the curves for $N = 24$ fall below the $N = 26$ curves at $l_{\max} = 7$. This corresponds perfectly to the claim that this 24 point layout is a 7-design, whereas the next 26 point set is only a 6-design (this means that the 24 point layout should be able to exactly reproduce the integration of polynomials up to an order of 7, whereas the 26 point layout is only exact for polynomials of a lower order, namely 6). We could observe an excellent correlation of these and similar curves with the claimed strengths of the layouts of Hardin and Sloane [26].

It is interesting to point out that Fliege and Maier [27] arrive at their number of points from the requirement of linear polynomial space to be $(m+1)^2$ for S_2 , where m is an integer. They have published cubature formula for 4, 9, 16, 25, ..., $(m+1)^2$, ..., 900 points. Spherical harmonics expansions up to an order of l_{\max} have $\sum_{l=0}^{l_{\max}} (2l+1)$ coefficients. As $\sum_{l=0}^{l_{\max}} (2l+1) = (l_{\max}+1)^2$, the number of spherical harmonics coefficients is the dimension of the polynomial space and equal to the number of nodes needed for integration on the

sphere. This restriction is not necessary for spherical t -designs: Hardin and Sloane [26] present a 216 point layout with equal weights that they claim is a 20-design. Based on the dimension of polynomial space, an integration layout would require $(20+1)^2 = 441$ points. Note that this number is still far smaller than the typically many thousand points required by a robust least-squares fit to this degree of l .

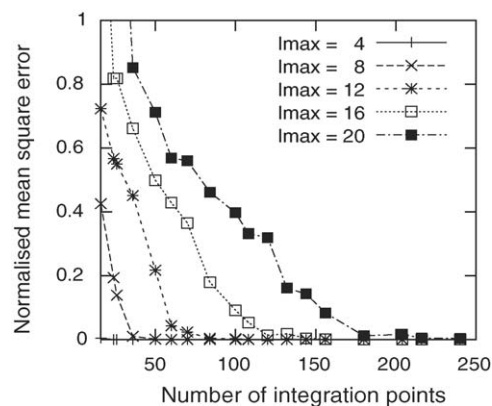


Fig. 5. The integration quality as a function of the number of sample points for various orders of spherical harmonic expansions. Given an acceptable average error tolerance such plots allow one to choose the optimal integration layout.

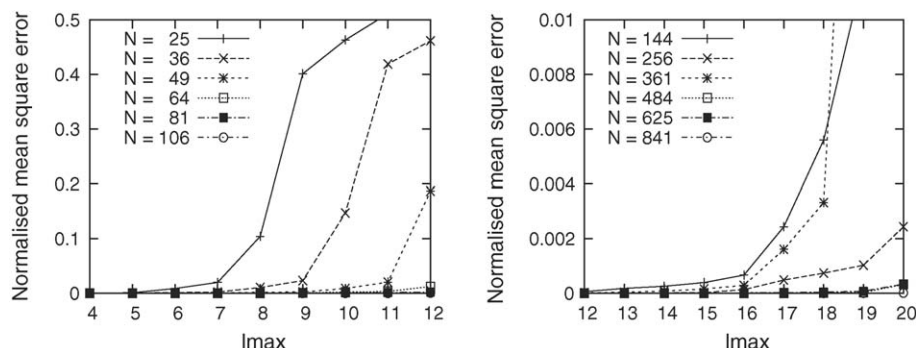


Fig. 6. The quality of the cubature formulae of Fliege and Maier [27] for spherical harmonic expansions for the small molecule NAD. The normalised mean square error between the original surface of degree l_{\max} and the reconstructed surface from a spherical harmonics expansion using various cubature formulae is shown. The large point sets achieve a very impressive degree of accuracy and compared to standard integration methods with a relatively small number of points.

4. Discussion

The computation of spherical harmonic expansion coefficients requires integration over the full surface of the sphere. The work in this manuscript extends ideas presented by Ritchie and Kemp [4]. Their icosahedron integration layout for spherical harmonic expansion coefficients led to around a third fewer sample points compared to an equi-angular grid. The use of well-researched cubature formulae for the determination of molecular surfaces using spherical harmonics can make significant savings in computation as compared to previous approaches: the integration layout with the integration weights doesn't need to be computed for every new case and the integration can take place with far fewer sample points than other approaches. In addition, this approach was more accurate in our hands than our own versions of icosahedron subdivision, surface triangularization, Voronoi region and common Monte Carlo integration methods. See Table 1, which gives the results for the data in Fig. 5. It must be pointed out that many of the listed error estimates are only meant to roughly capture the

expected behaviour of a single integral evaluation and do not represent strict upper boundaries. For Vegas Monte Carlo and Gauss-Legendre quadrature, the error estimate is zero only for sufficient sampling with the correct integration weights—we were not able to reproduce this with standard implementations for spherical harmonics reconstructions to $l_{\max} = 10$ and higher. Naturally, the integration quality depends strongly on the number of roots of the function on the sphere (high-order spherical harmonics, therefore, require a large number of points that often give rise to inaccuracies). Also this table neglects the additional computational cost of calculating integration weights and the overhead of adaptive schemes.

If spherical harmonics expansions are required of limited order of about $l_{\max} < 20$ then the spherical t -designs of Hardin and Sloane [26] present an elegant and extremely fast way of performing the integration for the computation of the expansion coefficients. Likewise for the cubature formulae of Fliege and Maier [27], which give good results on average and extend slightly further, but at a cost of a higher number of points at high l_{\max} to achieve a similar accuracy. Other techniques include the first and second Neumann method, Lebedev integration schemes, and Fibonacci Number layouts. Especially, the latter two may provide an attractive alternative to spherical designs for higher order expansions. Gauss-Legendre Quadrature should theoretically require in the order of 30% more points than techniques such as Fibonacci. The number of sample points for the cubature formulae is in the order of 10^2 , whereas other techniques are often several orders of magnitude higher, 10^4 – 10^6 . For expansion orders much above $l_{\max} > 20$, the proposed method lacks point layouts of a sufficient number of nodes and one must, therefore, fall back on other, computationally more intense integration procedures. Cubature formulae and error estimates for interpolation and integration remain under active research in many areas of applied mathematics.

5. Conclusions

We have used known theorems and results from sphere packing and coding theory and applied them with success to the computation of molecular surfaces. We have shown that

Table 1
A comparison of some integration techniques

Method	Error Estimate	$N_{l_{\max}=10, \varepsilon < 10^{-5}}$
Monte Carlo (Standard)	$N^{-1/2}$	$> 10^6$ (failed)
Monte Carlo (Mises)	$\frac{1}{2}N^{-1/2}$	$> 10^6$ (failed)
Monte Carlo (Vegas)	0	$> 10^6$ (failed)
Least squares (Simpson grid)	N^{-2}	64800
Gauss-Legendre quadrature	0	14400
Icosahedron subdivision	?	2562
Spherical designs	?	361
Spherical t -designs	0	156

This table lists some common integration methods with an estimated error as a function of the number of integration nodes N (? indicates that we were not able to find a suitable formula). With a sufficient number of sample points and the optimal integration weights some methods should be exact. The last column gives the number of points required to produce a reconstructed surface that deviated less than ε (RMSD) from the original surface (a stricter requirement than for one single integration). We have used GNU GSL [31] libraries wherever possible or gone for a no-frills straightforward implementation in all cases, many of the below numbers could therefore possibly be significantly improved upon, especially for those that are sensitive to integration weights.

molecular surfaces can be computed extremely efficiently using spherical harmonics and that the integrals can be approximated to a high degree of accuracy with a very limited number of sample points. The method of spherical designs thus has wide applications in many areas of molecular graphics and design for which integration of properties on the surface is required. Especially—but not only—applications involving spherical harmonics should benefit from this approach and experience a significant speedup.

Acknowledgments

I would like to thank Gérard Bricogne for introducing me to sphere packing, coding theory and spherical *t*-designs. I thank Lora Mak for critical reading of the manuscript. I am grateful to two anonymous referees for their questions and comments.

References

- [1] B. Ma, M. Shatsky, H.J. Wolfson, R. Nussinov, Multiple diverse ligands binding at a single protein site: a matter of pre-existing populations, *Protein Science* 11 (2002) 184–197.
- [2] N. Max, E.D. Getzoff, Spherical harmonic molecular surfaces, *IEEE Computer Graphics & Applications* 8 (1988) 42–50.
- [3] B.S. Duncan, A.J. Olson, Shape analysis of molecular surfaces, *Biopolymers* 33 (1993) 219–229.
- [4] D.W. Ritchie, G.J.L. Kemp, Fast Computation, Rotation, and comparison of low resolution spherical harmonic molecular surfaces, *J. Comp. Chem.* 20 (4) (1999) 383–395.
- [5] D.W. Ritchie, G.J.L. Kemp, Protein docking using spherical polar Fourier correlations, *Proteins: Struct. Funct. Genet.* 39 (4) (2000) 178–194.
- [6] W. Cai, X. Shao, B. Maigret, Protein-ligand recognition using spherical harmonic molecular surfaces: towards a fast efficient filter for large virtual throughput screening, *J. Mol. Graph. Model.* 20 (2002) 313–328.
- [7] R.J. Morris, R. Najmanovich, A. Kahraman, J.M. Thornton, Real spherical harmonic expansion coefficients as 3D shape descriptors for protein binding pocket and ligand comparisons, *Bioinformatics* 15 (2005) 2347–2355.
- [8] C. Cohen-Tannoudji, B. Dui, F. Laloë, *Quantum Mechanics*, vols. 1/2, Wiley Interscience, 1977 ISBN: 0-471-16432-1 & 0-471-16434-8.
- [9] H. Stuhmann, Interpretation of small-angle scattering functions of dilute solution and gases. A representation of the structures related to a one-particle scattering function, *Acta Cryst.* A26 (1970) 297–306.
- [10] D. Svergun, Mathematical methods in small-angle scattering data analysis, *J. Appl. Cryst.* 24 (1991) 485–492.
- [11] A. Matheny, D.B. Goldgof, The use of three- and four-dimensional surface harmonics for rigid and nonrigid shape recovery and representation, *IEEE Trans. Pattern Anal. Machine Intell.* 17 (10) (1995) 967–981.
- [12] R.A. Crowther, M.G. Rossmann, *The Fast Rotation Function*, The Molecular Replacement Method, Gordon & Breach, New York, 1972 pp. 173–178.
- [13] R.J. Morris, G. Bricogne, Sheldrick's 1.2 Å rule and beyond, *Acta Cryst.* D59 (2003) 615–617.
- [14] V.G. Tsirelson, R.P. Ozerov, *Electron Density and Bonding in Crystals*, Institute of Physics Publishing, 1996 ISBN: 0 7503 0284 4, pp 147–167.
- [15] J. Navaza, On the computation of the fast rotation function, *Acta Cryst.* D49 (1993) 588–591.
- [16] R.J. Morris, A. Kahraman, J.M. Thornton, Binding pocket shape analysis for protein function prediction, *Acta Cryst.* D61 (2005) C156–C157.
- [17] R.J. Morris, A. Kahraman, T. Funkhouser, R. Najmanovich, G. Stockwell, F. Glaser, R. Laskowski, J.M. Thornton, Binding pocket shape analysis for protein function prediction. in: S. Barber, P.D. Baxter, K.V. Mardia, R.E. Wells (Eds.), *Quantitative Biology, Shape Analysis, and Wavelets*, Leeds University Press, Leeds, 2005, pp. 91–94. ISBN: 0 85316 243 3.
- [18] T. Funkhouser, F. Glaser, R. Laskowski, R.J. Morris, R. Najmanovich, G. Stockwell, J.M. Thornton, Shape-based classification of bound ligands. in: S. Barber, P.D. Baxter, K.V. Mardia, R.E. Wells (Eds.), *Quantitative Biology, Shape Analysis, and Wavelets*, Leeds University Press, Leeds, 2005, pp. 39–42. ISBN: 0 85316 243 3.
- [19] A. Kudlicki, M. Rowicka, M. Gilski, Z. Otwinowski, An efficient routine for computing symmetric real spherical harmonics for high orders of expansion, *J. Appl. Cryst.* 38 (2005) 501–504.
- [20] D.W. Ritchie, High-order analytic translation matrix elements for real-space six-dimensional polar Fourier correlations, *J. Appl. Cryst.* 38 (2005) 808–818.
- [21] F. Pavelcik, J. Zelinka, Z. Otwinowski, Methodology and applications of automatic electron-density map interpretation by six-dimensional rotational and translational search for molecular fragments, *Acta Cryst.* D 58 (2002) 275–283.
- [22] W.H. Press, S.A. Teukolsky, W.T. Vetterling, B.P. Flannery, *Numerical Recipes in C*, Cambridge University Press, 1992.
- [23] K. Jetter, J. Stöckler, J.D. Ward, Norming sets and spherical cubature formulas, in: Z. Chen, Y. Li, C.A. Micchelli, Y. Xu (Eds.), *Computational Mathematics*, Marcel Dekker, Inc., New York, 1998, pp. 237–245, ISBN: 0-8247-1946-8.
- [24] G. Bricogne, Efficient Sampling Methods for Combinations of Signs, Phases, Hyperphases, and Molecular Orientations, *Methods in Enzymology, Macromolecular Crystallography, Part A*, vol. 276, Academic Press, 1997 ISBN: 0-12-182177-3, pp. 424–448.
- [25] J.-M. Goethals, J.J. Seidel, Spherical designs, in: D.K. Ray-Chaudhuri (Ed.), *Relations between Combinatorics and Other Parts of Mathematics*, *Proc. Symp. Pure Math.*, vol. 34, 1979, pp. 255–272.
- [26] R.H. Hardin, J.A. Sloane, McLaren's improved snub cube and other new spherical designs in three dimensions, *Discrete and Computational Geometry* 15 (1996) 429–441.
- [27] J. Fliege, U. Maier, A two-stage approach for computing cubature formulae for the sphere. Technical Report. *Ergebnisberichte Angewandte Mathematik* 139T, Universität Dortmund, Fachbereich Mathematik, 1996.
- [28] J.R. Morris, D.M. Deaven, K.M. Ho, Genetic-algorithm energy minimization for point charges on a sphere, *Phys. Rev. B* 54 (4) (1996) 1740–1743.
- [29] R. Meijers, R.J. Morris, H.W. Adolph, A. Merli, V.S. Lamzin, E.S. Cedergren-Zeppeauer, On the enzymatic activation of NADH, *J. Biol. Chem.* 276 (2001) 9316–9321.
- [30] A. Schmidt, A. Gonzalez, R.J. Morris, M. Costabel, P.M. Alzari, V.S. Lamzin, Advantages of high-resolution phasing: MAD to atomic resolution, *Acta Cryst.* D 58 (2002) 1433–1441.
- [31] M. Galassi, J. Davies, J. Theiler, B. Gough, G. Jungman, M. Booth, F. Rossi, *GNU Scientific Library Reference Manual* (2nd), ISBN: 0-9541617-3-4, 2003.
- [32] W.L. DeLano, *The PyMOL Molecular Graphics System*, 2002. World Wide Web <http://www.pymol.org>.